Frontiers in Bioscience Landmark

Front. Biosci. (Landmark Ed) **2025**; 30(10): 45454
https://doi.org/10.31083/FBL45454

Original Research

Study on the Mechanism of CCN2 Promoting Sorafenib Resistance in HCC and Its Combined Intervention Strategy

Lei Cui[1,2,†], Junhao Liu[1,2,†], Yongxue Lv[3], Bendong Chen[1,2], Kejun Liu[1,2,*], Yang Bu[1,2,*]

[1]Department of Hepatobiliary Surgery, General Hospital of Ningxia Medical University, 750004 Yinchuan, Ningxia, China
[2]School of Clinical Medicine, Ningxia Medical University, 750004 Yinchuan, Ningxia, China
[3]School of Basic Medicine, Ningxia Medical University, 750004 Yinchuan, Ningxia, China
*Correspondence: kejun_liu1994@163.com (Kejun Liu); boyang1976@163.com (Yang Bu)
[†]These authors contributed equally.

Academic Editors: Graham Pawelec and Amancio Carnero Moya
Submitted: 31 July 2025 Revised: 12 October 2025 Accepted: 15 October 2025 Published: 31 October 2025

Abstract

Background: Since its introduction in 2008, sorafenib has remained the standard first-line systemic treatment for advanced hepatocellular carcinoma (HCC). Nevertheless, its clinical benefits are often compromised by the rapid emergence of drug resistance. This study explores the molecular mechanisms underlying sorafenib resistance, with particular emphasis on the involvement of connective tissue growth factor (CCN2/CTGF) in the regulation of c-Met signaling pathways. **Methods**: We began by evaluating CCN2 expression levels in HCC tissue samples via immunohistochemistry and analyzing their correlation with clinicopathological characteristics. To functionally characterize CCN2, we established stable HCC cell lines with either knockdown or overexpression of the gene using lentiviral transduction. The effects of CCN2 on cellular proliferation and drug resistance were evaluated using cell counting kit-8 (CCK-8) and colony formation assays. To elucidate the downstream signaling mechanisms, a tyrosine kinase PCR array was employed to identify expression changes within the tyrosine kinase superfamily after CCN2 knockdown. Further investigation into the molecular mechanism by which CCN2 promotes sorafenib resistance was conducted using real-time quantitative PCR (RT-qPCR), western blotting, and immunofluorescence. Finally, the therapeutic potential of co-targeting CCN2 and sorafenib was validated in a nude mouse xenograft tumor model. **Results**: Our results establish that CCN2 overexpression significantly enhances HCC proliferation, while also inducing resistance to sorafenib. Mechanistically, we identified that CCN2 binds to integrin αV, triggering focal adhesion kinase (FAK) phosphorylation, which in turn promotes yes-associated protein (YAP) nuclear translocation and leads to the transcriptional upregulation of c-Met. This proposed signaling axis was consistently supported by tyrosine kinase PCR array, co-immunoprecipitation, and western blot analyses. Ultimately, *in vivo* experiments confirmed that simultaneously targeting CCN2 and administering sorafenib produces a synergistic effect, markedly inhibiting tumor growth and restoring therapeutic sensitivity. **Conclusion**: These results not only elucidate a novel CCN2/FAK/YAP/c-Met axis in sorafenib resistance but also provide a mechanistic rationale for dual-targeting strategies to improve outcomes in advanced HCC.

Keywords: hepatocellular carcinoma; connective tissue growth factor; c-Met; sorafenib; drug resistance

1. Introduction

Hepatocellular carcinoma (HCC) presents a major global health challenge, being the sixth most commonly diagnosed cancer and the third leading cause of cancer-related deaths worldwide [1]. The burden of this disease is particularly acute in China, where it is the second deadliest malignancy, resulting in 316,500 annual fatalities and trailing only lung cancer [2,3]. This disparity is largely driven by the dual challenges of late diagnosis and limited treatment options for advanced disease. Although surgical resection can achieve five-year survival rates of 50–60% in early-stage HCC, over 80% of Chinese patients are diagnosed at an advanced stage, often due to a high background prevalence of hepatitis B/C-induced cirrhosis. Consequently, more than 60% of patients are limited to palliative care options, primarily including transarterial chemoembolization (TACE) or tyrosine kinase inhibitors [4–6].

While the tumor microenvironment is increasingly recognized as a critical factor in HCC pathogenesis—driving hepatic fibrogenesis, epithelial-mesenchymal transition, and metastasis—current therapeutic strategies remain predominantly focused on directly targeting tumor cells, leaving microenvironmental modulation as a relatively unexplored avenue. This gap in focus likely contributes to the persistently poor prognosis of advanced HCC [7,8]. Within this specialized niche, bidirectional tumor-stroma interactions facilitate tumor progression, with CCN family proteins acting as key mediators. Among them, CCN2, a cysteine-rich matricellular protein, plays multifunctional roles in regulating cell migration, angiogenesis, and proliferation [9,10]. Research has established that CCN2 plays a significant role in multiple aspects of tumor progression—including growth, migration, invasion, angiogenesis, and drug resistance—in cancers such as breast

cancer, osteosarcoma, prostate cancer, and hepatocellular carcinoma [11–14]. Its involvement in chemoresistance has become a key research focus. For instance, CCN2 was reported to enhance doxorubicin resistance in osteosarcoma by upregulating ATP-binding cassette subfamily G member 2 (ABCG2) expression [15], while epigallocatechin-3-gallate was shown to reduce osimertinib resistance in non-small cell lung cancer by targeting CCN2. In glioblastoma, CCN2 promotes temozolomide resistance via TGF-β1-dependent Smad/ERK signaling [16]. In HCC, elevated CCN2 expression has been preliminarily associated with poor patient prognosis. Similarly, our previous work demonstrated that CCN2 significantly contributes to oxaliplatin resistance through interactions with receptors including LRP6, integrins, and c-Met [17], underscoring its importance in HCC malignancy and therapy resistance. However, the role and underlying mechanisms of CCN2 in mediating sorafenib resistance in hepatocellular carcinoma remain unexplored.

The c-Met tyrosine kinase receptor, encoded by the Mesenchymal Epithelial Transition Factor (MET) proto-oncogene, has emerged as a key therapeutic target in oncology. As the principal receptor for hepatocyte growth factor (HGF), it orchestrates critical oncogenic processes including cytoskeletal remodeling, tumor proliferation, and chemoresistance [18,19]. Clinical observations correlate c-Met overexpression with aggressive tumor phenotypes and therapeutic resistance across multiple malignancies [20,21]. Notably, while CCN2-c-Met interactions have been implicated in HCC drug resistance, their precise mechanistic contributions require further elucidation.

The Food and Drug Administration (FDA) approval of sorafenib in 2008 marked a milestone in the treatment of advanced HCC. However, the clinical benefits of this multi-kinase inhibitor are often curtailed by the rapid development of resistance [22]. Based on existing evidence of chemoresistance mechanisms, we propose that CCN2-mediated activation of the c-Met pathway may be a key driver of sorafenib resistance in CCN2-overexpressing HCC. Therefore, this study systematically examines the link between CCN2 expression and malignant progression, and evaluates its role in modulating sorafenib sensitivity. By combining CCN2 inhibition with sorafenib in experimental models, we delineate the molecular mechanism of this resistance via the CCN2/c-Met axis. Our integrated approach aims to provide a preclinical rationale for novel combination strategies that target CCN2 signaling to improve sorafenib efficacy in HCC.

2. Materials and Methods

2.1 Clinical Samples

This retrospective study utilized archived paraffin-embedded tissue specimens and clinical records from 60 HCC patients who underwent surgical resection at the General Hospital of Ningxia Medical University between 2019 and 2022. Patient inclusion required: (1) postoperative pathological confirmation of HCC, (2) no history of prior anticancer therapy, (3) availability of complete clinical data, and (4) procurement of both tumor and adjacent normal tissue samples (located $>$2 cm from the tumor margin). Exclusion criteria comprised a diagnosis of other concurrent malignancies or significant cardiovascular/respiratory comorbidities. The research was approved by the Medical Research Ethics Review Committee of the General Hospital of Ningxia Medical University (No. KYLL-2019-080). A written consent was signed by the patients or their families/legal guardians.

2.2 Antibodies

Antibodies included CCN2 (ab6992, Abcam, Cambridge, Cambridgeshire, UK); β-actin (ab8226, abcam, Cambridge, Cambridgeshire, UK); c-Met (8198T, Cell Signaling Technology, Danvers, MA, USA); p-Met (3077T, Cell Signaling Technology, Danvers, MA, USA); IntegrinαV (3019, Cell Signaling Technology, Danvers, MA, USA); FAK (3285, Cell Signaling Technology, Danvers, MA, USA); p-FAK (3283, Cell Signaling Technology, Danvers, MA, USA); YAP (14074, Cell Signaling Technology, Danvers, MA, USA); and p-YAP (13008, Cell Signaling Technology, Danvers, MA, USA).

2.3 Immunohistochemistry

Paraffin-embedded tissue sections underwent sequential deparaffinization using xylene gradients and rehydration through graded ethanol series. Antigen retrieval was achieved through microwave irradiation in sodium citrate buffer (pH 6.0), followed by natural cooling to room temperature. The staining protocol included three cycles of PBS washing (5 min each), endogenous peroxidase inactivation with 3% H_2O_2 (10 min, room temperature), and non-specific binding blockage using 5% BSA (30 min, RT). Primary antibody incubation was performed at 4 °C overnight, followed by HRP-conjugated secondary antibody (1:200) treatment for 1 h at room temperature. Signal visualization employed 3,3′-Diaminobenzidine (DAB) chromogenic substrate with hematoxylin counterstaining, culminating in ethanol dehydration, xylene clearing, and neutral resin mounting. Two blinded pathologists independently evaluated staining outcomes using a semi-quantitative scoring system: (1) Positive cell proportion: 1 ($\leq$25%), 2 (26–50%), 3 (51–75%), 4 ($>$75%); (2) Staining intensity: 0 (negative), 1 (weak), 2 (moderate), 3 (strong). Final scores (range: 0–12) were calculated by multiplying proportion and intensity scores. Specimens were stratified into low-expression ($<$median score) and high-expression ($\geq$median score) cohorts.

2.4 Cell Culture and Transfection

Cell lines including MHCC97L, MHCC97H, HCCLM3, Hep3B, Huh-7, and LO2 were all kindly provided by the Liver Disease Research Institute affiliated with Fudan University in Shanghai. These cells were cultured

Table 1. Primer sequences used for RT-qPCR.

Gene		Primer sequences (5′-3′)
CCN2	Forward	CTGTGGAGTATGTACCGACGGCC
	Reverse	ATGGCAGGCACAGGTCTTGATGAAC
MET	Forward	GTGAATTAGTTCGCTACGATGC
	Reverse	GTCAGAGGATACTGCACTTGTCG
GAPDH	Forward	GGCAAATTCCATGGCACCGTCAAGG
	Reverse	GCCAGCATCGCCCCACTTGATTTTG

RT-qPCR, real-time quantitative polymerase chain reaction; *CCN2*, Cellular Communication Network Factor 2; *MET*, Mesenchymal-Epithelial Transition Factor; *GAPDH*, Glyceraldehyde-3-Phosphate Dehydrogenase.

in Dulbecco's modified Eagle medium (DMEM, 2329225, VivaCell, Shanghai, China) supplemented with 10% fetal bovine serum (FSP500, ExCell Bio, Shanghai, China) and 1% penicillin-streptomycin (P1400, Solarbio, Beijing, China). All cells were maintained at 37 °C with 5% CO_2. All cell lines used in this study were authenticated by short tandem repeat (STR) profiling and confirmed to be mycoplasma-negative. Lentiviruses for CCN2 overexpression and knockdown were purchased from Beijing Tsingke Biotech Co., Ltd. (China). Lentiviral transfections were conducted according to the manufacturer's instructions, with Lipo3000 (L3000015, Invitrogen, Carlsbad, CA, USA) used as recommended. Screening was performed using puromycin (P8230, Solarbio, Beijing, China).

2.5 Real-Time Quantitative Polymerase Chain Reaction (RT-qPCR)

Total RNA was extracted from cells using the MolPure® Cell/Tissue Total RNA Kit (19221ES50, Yeasen Biotechnology, Shanghai, China), and cDNA was synthesized using the PrimeScript™ RT Master Mix (Perfect Real Time) (RR036A, Takara Bio, Kyoto, Japan). Subsequently, RT-qPCR reactions were performed using the TB Green® Premix Ex Taq™ RNaseH Plus kit (RR820A, Takara Bio, Kyoto, Japan). The primers (Table 1) used in this study were designed and synthesized by Tsingke Biotech Co., Ltd. (Beijing, China).

2.6 Western Blot

Protein extraction from hepatic carcinoma specimens and cultured cells was performed using radioimmunoprecipitation (RIPA) lysis buffer (P0013B, Beyotime Biotechnology, Shanghai, China) supplemented with protease/phosphatase inhibitors. After 20-min ice incubation, lysates were clarified by centrifugation (12,000 ×g, 10 min, 4 °C) to remove insoluble components. Protein quantification was conducted via bicinchoninic acid (BCA) assay (KGB2101-100, KeyGEN BioTECH, Nanjing, Jiangsu, China) with bovine serum albumin as standard. Equal amounts of protein (30 µg/lane) were resolved on 10% SDS-polyacrylamide gels and electrophoretically transferred to polyvinylidene fluoride (PVDF) membranes. Membranes were blocked with 5% BSA or non-fat milk (1 h, RT) prior to overnight incubation with primary antibodies (4 °C). Following three TBST (Tris-buffered saline, 0.1% Tween 20) washes, membranes were probed with species-matched HRP-conjugated secondary antibodies (1:5000, 1 h, RT). Subsequent to additional TBST rinses, chemiluminescent signals were developed using ECL Plus substrate (PE0010, Solarbio, Beijing, China) and quantified with the Tanon-5200 automatic chemiluminescence imaging analysis system (Tanon, Shanghai, China).

2.7 Transwell Assay

In the lower chamber of a Transwell insert (16122062, Corning, New York, NY, USA), 500 µL of DMEM containing 10% fetal bovine serum was added, while 200 µL of DMEM containing 8×10^4 cells was added to the upper chamber. Following 48 h of incubation, the inserts were removed, fixed with 4% paraformaldehyde for 15 min, and stained with 0.1% crystal violet for 30 min. Images were captured using an inverted microscope (DMi8, Leica, Wetzlar, Hesse, Germany), and the number was counted using ImageJ software (version 1.8.0, National Institutes of Health, Bethesda, MD, USA).

2.8 Wound-Healing Assay

Hepatocellular carcinoma cells were plated in six-well plates and cultured to confluence, while wounds were inflicted using a 200 µL pipette tip. After removing cell debris with PBS, cells were cultured in serum-free medium. Wound closure was monitored using an inverted microscope (DMi8, Leica, Wetzlar, Hesse, Germany) every 0 and 24 h.

2.9 Cell Proliferation Assay

Cell proliferation was assessed using the Cell Counting Kit-8 (B34304, Biomake, Beijing, China). HCC cells were seeded in 96-well plates at a density of 2000 cells per well and cultured at 37 °C for 12, 24, 48, 72, and 96 h, respectively. Each well was subsequently treated with 10 µL of CCK-8 solution and 100 µL of DMEM. Upon incubation for 2 h, absorbance was measured at 450 nm using a microplate reader (Multiskan SkyHigh, Thermo Scientific, Waltham, MA, USA).

2.10 Colony Formation Assay

Hepatocellular carcinoma cells were seeded in 6-well plates at a density of 500 cells per well. After 14 d of culture, the cells were fixed with 4% paraformaldehyde for 15 min, washed three times with PBS, and stained with 0.1% crystal violet for 30 min. Afterwards, the number of colonies was counted using ImageJ software (version 1.8.0, National Institutes of Health, Bethesda, MD, USA).

2.11 Detection of Sorafenib IC_{50} in HCC Cell Lines

Cells were seeded into 96-well plates at a density of 5000 cells per well and incubated. Once the cells adhered,

varying concentrations of Sorafenib (0 μM, 1.25 μM, 2.5 μM, 5 μM, 10 μM, 20 μM, 40 μM, and 80 μM) were added according to the experimental groups. Upon further incubation for 24 h, CCK-8 solution was added, the absorbance at 450 nm was measured, and cell viability was calculated.

2.12 Data Collection and Enrichment Analysis

RNA-seq data for HCC were obtained from The Cancer Genome Atlas (TCGA) database (https://portal.gdc.cancer.gov/). Based on the median expression level of CCN2, HCC patients were categorized into high-expression (n = 187) and low-expression (n = 187) groups, and differentially expressed genes between these two groups were identified. The resulting CCN2-associated differentially expressed genes were subsequently analyzed and functionally enriched using the GSEA platform (https://www.gsea-msigdb.org/gsea/index.jsp). Transcription factors potentially regulating the c-Met gene were predicted via the humanTFDB database. Finally, Kyoto Encyclopedia of Genes and Genomes (KEGG) pathway enrichment analysis was conducted on these c-Met-related transcription factors using The Database for Annotation, Visualization and Integrated Discovery (DAVID) database (https://davidbioinformatics.nih.gov/summary.jsp). The correlation between Met and Yap expression was analyzed using the Gene Expression Profiling Interactive Analysis (GEPIA) database (http://gepia.cancer-pku.cn/).

2.13 Co-Immunoprecipitation (Co-IP)

Protein complexes were isolated using Protein A/G Magnetic Beads (88802, Thermo Scientific, Carlsbad, CA, USA) according to manufacturer specifications. For antibody conjugation, 20 μL bead suspension was incubated with either control IgG (2729, Cell Signaling Technology, Danvers, MA, USA) or CCN2-specific antibody (50 μg/mL final concentration, ab6992, Abcam, Cambridge, Cambridgeshire, UK) under rotary agitation (25 °C, 1 h). Following magnetic separation (800 ×g, 30 sec) and three wash cycles with PBS-0.1% Tween, pre-cleared cellular/tissue lysates were introduced for target protein capture (4 °C, overnight rotation). Sequential purification steps included: ① Four cycles of binding/wash buffer treatment with magnetic separation. ② Two washes with 20 bead-bed volumes of Tris-buffered saline (TBS, pH 7.4). ③ Acidic elution using 0.1 M glycine-HCl (pH 3.5, ≤20 min incubation).

Eluted proteins were denatured in 5× Laemmli buffer (95 °C, 10 min) prior to immunoblotting analysis. This optimized protocol maintained protein complex integrity while effectively reducing non-specific binding, achieving >85% capture efficiency as validated by tandem mass spectrometry.

2.14 Immunofluorescence

Cells were plated in 24-well plates with cover slips and cultured to 50%–70% confluence. The medium was removed, and cells were washed three times with PBS, fixed with 4% paraformaldehyde at room temperature for 20 min, and washed again three times with PBS. Cells were then permeabilized with 0.3% Triton X-100 for 20 min, blocked with 5% BSA for 1 h, and incubated with primary antibodies overnight at 4 °C. Following this, cells were incubated with fluorescent secondary antibodies for 1 h at room temperature, stained with DAPI for nuclear counterstaining, and mounted. Images were captured using a fluorescence inverted microscope (DMi8, Leica, Wetzlar, Hesse, Germany) .

2.15 Animal Experiments

Female BALB/c-nu nude mice (4–5 weeks old) were obtained from Beijing Vital River Laboratory Animal Technology Co., Ltd. and housed under specific pathogen-free (SPF) conditions. Subcutaneous xenograft models were established by injecting 150 μL of a cell suspension containing 5×10^6 cells into the left axilla of each mouse. On day 30 post-inoculation, mice were humanely euthanized through a two-stage procedure: initial anesthesia was induced with isoflurane inhalation (4% in oxygen), followed by an intraperitoneal injection of sodium pentobarbital (100 mg/kg) to ensure cardiac arrest. Death was confirmed by the cessation of circulatory function via venous puncture. The tumors were then excised, and their volume (calculated as $0.5 \times \text{length} \times \text{width}^2$), weight, and macroscopic appearance were recorded. All experimental procedures involving animals were performed in strict accordance with the National Institutes of Health guidelines for the care and use of laboratory animals and were approved by the Medical Research Ethics Review Committee of the General Hospital of Ningxia Medical University (No. KLYY-2019-080).

2.16 Statistical Analysis

Statistical analysis and graphical presentation were conducted using SPSS (version 26.0, IBM, Armonk, NY, USA) and GraphPad Prism (version 8.0, San Diego, Boston, MA, USA). For quantitative data following a normal distribution, comparisons between two groups were made using *t*-tests, and comparisons among multiple groups were performed using analysis of variance (ANOVA). The association between CCN2 and clinical pathological characteristics was further assessed using *t*-tests, Wilcoxon rank-sum tests, chi-square tests, and Fisher's exact tests, with $p < 0.05$ indicating statistical significance.

3. Results

3.1 Biological Functions and Clinical Significance of CCN2 in HCC

Clinical data and specimens from 60 HCC patients treated at the General Hospital of Ningxia Medical University between 2019 and 2022 were analyzed in this study. Immunohistochemical analysis localized CCN2 predominantly to the cytoplasm of HCC cells (Fig. 1A). This study investigated the correlation between CCN2 expres-

sion levels and the clinicopathological characteristics of HCC patients in a real-world study (Table 2). The results revealed that CCN2 expression was significantly associated with a history of hepatitis B, aspartate aminotransferase (AST) levels, the severity of liver cirrhosis, and tumor size ($p < 0.05$). Consistent with these clinical findings, Western blot analysis revealed differential CCN2 protein expression across hepatocellular carcinoma cell lines. Specifically, CCN2 expression was markedly elevated in Hep3B and Huh-7 cell lines compared to the normal hepatic LO2 cell line (Fig. 1B). To investigate the functional role of CCN2, we generated stable CCN2-overexpressing LM3 cells and CCN2-knockdown Hep3B/Huh-7 cells using lentiviral transduction. The efficiency of genetic manipulation was confirmed at both the protein and transcript levels by Western blot (Fig. 1C) and RT-qPCR (Fig. 1D), respectively. CCK-8 and colony formation assays demonstrated that CCN2 knockdown significantly suppressed the proliferation of hepatocellular carcinoma cells, whereas CCN2 overexpression enhanced it (Fig. 1E,F). Similarly, Transwell migration assays revealed that CCN2 depletion inhibited cell migration (Fig. 1G), and wound healing assays confirmed that CCN2 overexpression promoted migratory capacity (Fig. 1H).

3.2 Effects of CCN2 Expression Changes on Sorafenib Resistance in Hepatocellular Carcinoma Cells in Vitro

The *in vitro* sensitivity of various hepatocellular carcinoma cell lines (MHCC97L, MHCC97H, HCCLM3, Huh-7, Hep3B) and the normal LO2 cell line to sorafenib was assessed, yielding IC_{50} values of 16.92, 21.76, 17.42, 11.66, 10.48, and 14.84 µM, respectively (Fig. 2A). Subsequent experiments demonstrated that CCN2 overexpression in HCCLM3 cells increased the sorafenib IC_{50} (CON vs. OV: 16.95 vs. 23.29 µM, $p < 0.001$), whereas CCN2 knockdown in Hep3B cells decreased it (shCON vs. sh#3: 10.91 vs. 7.293 µM, $p < 0.001$) (Fig. 2B), indicating that CCN2 downregulation enhances sorafenib sensitivity. This conclusion was further supported by CCK-8 assays, in which combined CCN2 knockdown and sorafenib treatment significantly suppressed HCC cell proliferation ($p < 0.001$; Fig. 2C).

3.3 CCN2 Enhancing Sorafenib Resistance in Hepatocellular Carcinoma Cells via c-Met Signaling Activation

Sorafenib, the first FDA-approved multi-targeted tyrosine kinase inhibitor for advanced hepatocellular carcinoma, inhibits tumor growth primarily by suppressing angiogenesis. To identify potential mediators of resistance, a tyrosine kinase PCR array profiling 90 tyrosine kinases (60 receptor and 30 non-receptor types) was used in CCN2-knockdown Hep3B cells. This screen revealed a broad downregulation of tyrosine kinase mRNAs, most notably c-Met (Fig. 3A). Subsequent validation by RT-qPCR and Western blot confirmed that CCN2 knockdown specifically reduces c-Met expression at both the mRNA and protein levels (Fig. 3B,C). These findings indicate that CCN2 promotes sorafenib resistance in HCC cells, at least in part, through the activation of c-Met.

3.4 CCN2 Upregulating c-Met Expression in Hepatocellular Carcinoma Cells Through Integrin-Mediated FAK/YAP Pathway

To further elucidate the specific mechanisms of CCN2 regulating c-Met transcription, the HumanTFDB was hereby used to predict transcription factors of the c-Met gene, and the DAVID database was employed for pathway enrichment analysis. The results indicated that the Hippo Signaling Pathway was involved in the transcriptional regulation of c-Met by CCN2 (Fig. 4A). Additionally, GSEA enrichment analysis showed significant enrichment of Hippo Signaling Regulation Pathways in populations with high CCN2 expression (Fig. 4B). The Hippo kinase pathway was identified as a carcinogenic resistance mechanism following many traditional small-molecule therapies, with YAP, a key transcriptional coactivator, translocating to the nucleus upon activation to regulate the transcription of downstream genes. The GEPIA database also demonstrated a positive correlation between YAP and c-Met expression (Fig. 4C). Additionally, subsequent immunofluorescence revealed that overexpression of CCN2 promoted YAP nuclear translocation, while CCN2 knockdown reduced YAP nuclear aggregation (Fig. 4D), demonstrating CCN2-mediated YAP nuclear translocation as a critical mechanism in regulating c-Met expression.

Following that, the mechanisms of CCN2 regulating YAP were investigated. Integrin subunit αV (Integrin αV), a component of integrins and a key target of CCN2, transmits signals from integrins to downstream targets via FAK, thereby promoting tumor progression. FAK also serves as a critical molecule mediating YAP nuclear translocation and transcriptional regulatory effects. In this study, to clarify the relationship between CCN2 and Integrin αV, co-immunoprecipitation (Co-IP) results confirmed that CCN2 bound to and interacted with Integrin αV (Fig. 4E). Western blot analysis showed that the phosphorylation levels of FAK decreased or increased correspondingly upon CCN2 knockdown or overexpression, while no significant changes were observed in Integrin αV expression (Fig. 4F). This suggested that Integrin αV might be activated upon binding to CCN2, thereby promoting the phosphorylation of downstream FAK. To test this hypothesis, the integrin inhibitor Cyclo(-RGDfK) was utilized to interfere with the activity of Integrin αV, and the results showed that Cyclo(-RGDfK) effectively reversed the activation of FAK by CCN2 (Fig. 4G).

To investigate the dependence of CCN2's regulation of c-Met on the Integrin αV/FAK/YAP axis, the activity of Integrin αV, FAK, and YAP was sequentially inhibited using the integrin inhibitor Cyclo(-RGDfK), the FAK inhibitor Defactinib, and the YAP inhibitor Verteporfin.

Table 2. The relationship between CNN2 expression levels and clinicopathological characteristics of patients with HCC in real-world study.

Characteristics	Expression of CCN2		Statistic	*p*-value
	Low (n = 29)	High (n = 31)		
Age (years)				
≤50	9 (50%)	9 (50%)	0.029	0.866
>50	20 (47.6%)	22 (52.4%)		
Gender				
Female	8 (57.1%)	6 (42.9%)	0.568	0.451
Male	21 (45.7%)	25 (54.3%)		
HBsAg, n (%)				
Positive	23 (42.6%)	31 (57.4%)	5.013	0.025
Negative	6 (100%)	0 (0%)		
AFP (ng/mL)				
<20	12 (66.7%)	6 (33.3%)	3.461	0.063
≥20	17 (40.5%)	25 (59.5%)		
TB (μmol/L)				
<40	29 (49.2%)	30 (50.8%)		1.000
≥40	0 (0%)	1 (100%)		
ALB (g/L)				
<40	17 (44.7%)	21 (55.3%)	0.537	0.464
≥40	12 (54.5%)	10 (45.5%)		
AST (U/L)				
<40	26 (72.2%)	10 (27.8%)	19.665	<0.001
≥40	3 (13%)	20 (87%)		
ALT (U/L)				
<40	21 (58.3%)	15 (41.7%)	2.636	0.104
≥40	8 (36.4%)	14 (63.6%)		
ALP (U/L)				
<135	26 (47.3%)	29 (52.7%)	0.006	0.938
≥135	3 (60%)	2 (40%)		
Degree of cirrhosis				
Mild	25 (73.5%)	9 (26.5%)	19.946	<0.001
Moderate & Severe	4 (15.4%)	22 (84.6%)		
Tumor size (cm)				
<5	21 (60%)	14 (40%)	4.578	0.032
≥5	8 (32%)	17 (68%)		
Microvascular tumor thrombus, n (%)				
No	15 (60%)	10 (40%)	2.336	0.126
Yes	14 (40%)	21 (60%)		
T stage, n (%)				
T1–T2	21 (55.3%)	17 (44.7%)	1.993	0.158
T3–T4	8 (36.4%)	14 (63.6%)		
Capsule of membrane				
No	17 (53.1%)	15 (46.9%)	0.442	0.506
Yes	12 (44.4%)	15 (55.6%)		
Vascular invasion				
No	13 (43.3%)	17 (56.7%)	0.601	0.438
Yes	16 (53.3%)	14 (46.7%)		

HCC, hepatocellular carcinoma.

Western blot analysis demonstrated that silencing CCN2 decreased the activity of FAK and YAP, as well as the expression of c-Met. In contrast, the addition of Cyclo(-RGDfK), Defactinib, and Verteporfin progressively suppressed the activity or expression of corresponding downstream molecules. Overexpression of CCN2 increased the activity of FAK and YAP, and the expression of c-Met, an effect effectively reversed by inhibiting the activity of Inte-

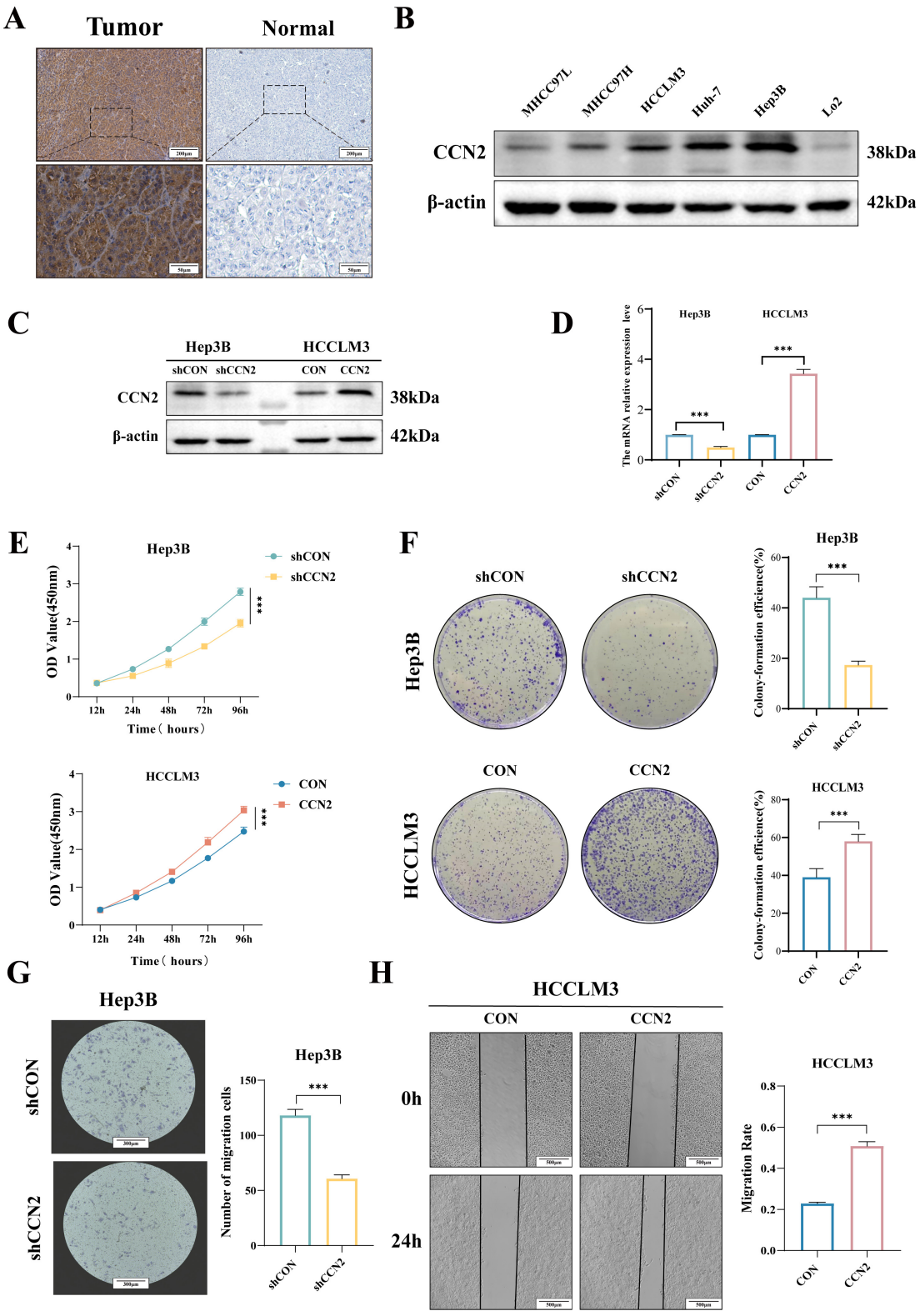

Fig. 1. Expression and biological functions of CCN2 in HCC. (A) Immunohistochemical assessment of CCN2 expression in hepatocellular carcinoma tissues. Scale bar: 200 μm (upper) and 50 μm (lower). (B) Western blot analysis of CCN2 expression levels in hepatocellular carcinoma cell lines. (C,D) Establishment of stable hepatocellular carcinoma cell lines with CCN2 overexpression and knockdown. (E,F) CCK-8 and colony formation assays to evaluate the effects of CCN2 on hepatocellular carcinoma cell proliferation and clonogenic potential. (G,H) Transwell and wound-healing assay to assess the effects of CCN2 on hepatocellular carcinoma cell migration. Scale bar: 300 μm (G) and 500 μm (H). Per group n = 3, ***$p < 0.001$.

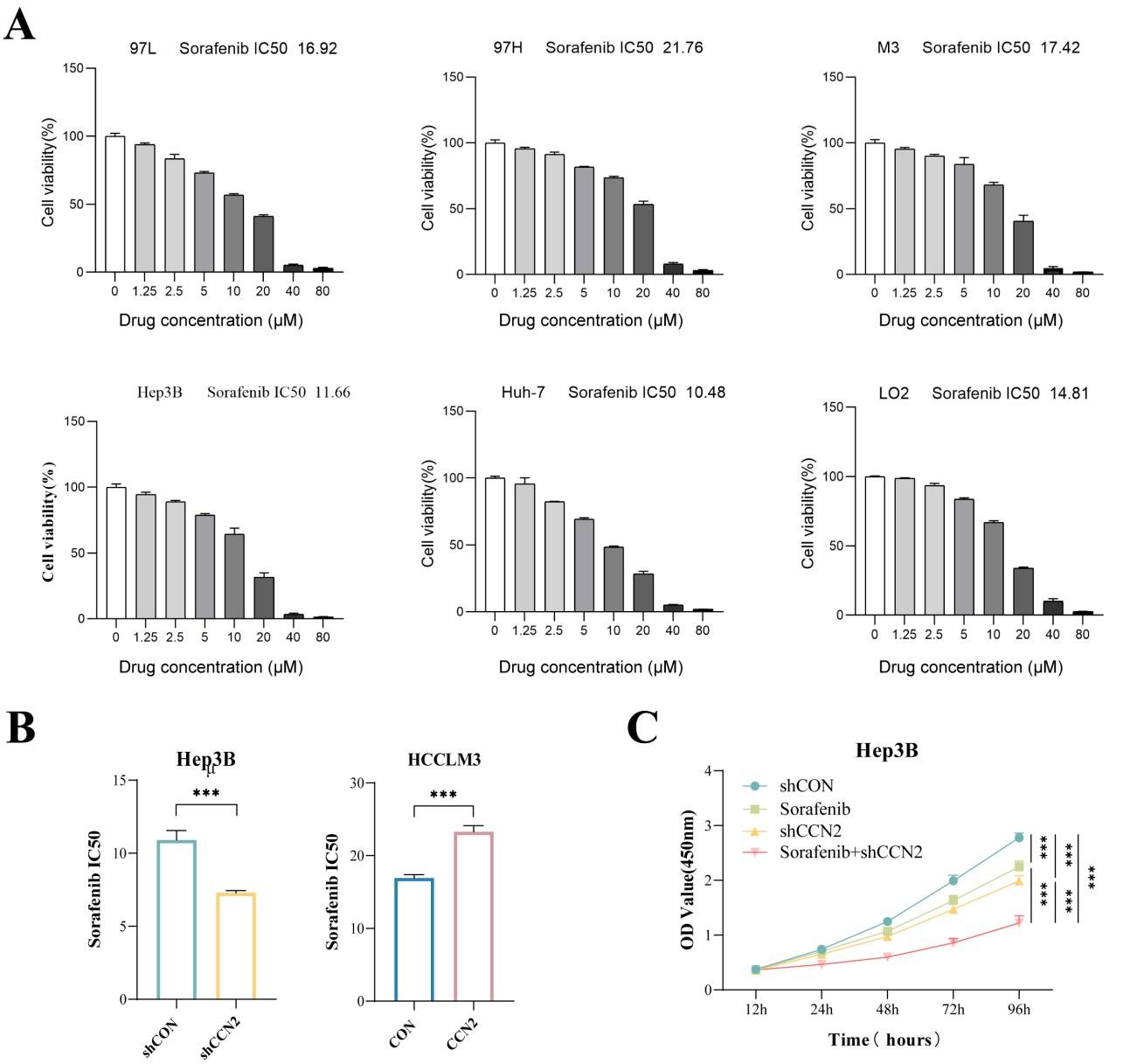

Fig. 2. Impact of CCN2 expression changes on sorafenib resistance in hepatocellular carcinoma cells *in vitro*. (A) Determination of sorafenib IC_{50} values in hepatocellular carcinoma cell lines MHCC97L, MHCC97H, HCCLM3, Huh-7, Hep3B, and the normal liver cell line LO2. (B) Assessment of sorafenib IC_{50} values in hepatocellular carcinoma cell lines with CCN2 knockdown or overexpression. (C) CCK-8 assay evaluating the effect of CCN2 knockdown combined with sorafenib on the proliferation of hepatocellular carcinoma cells. ***$p < 0.001$.

grin αV, FAK, and YAP (Fig. 4H,I). These results suggested that the secreted protein CCN2 bound to membrane receptors such as integrins to activate downstream FAK, which subsequently mediated the nuclear translocation of the transcriptional coactivator YAP, thereby enhancing the transcriptional activity of c-Met in hepatocellular carcinoma cells.

3.5 Enhanced Efficacy of Sorafenib in Liver Cancer Treatment Through CCN2 Interference

To investigate the role of CCN2 in promoting tumor growth *in vivo* and conferring resistance to sorafenib, Huh-7 cells with either control or CCN2 knockdown (assigned to shCON, shCCN2, shCON + Sorafenib, and shCCN2 + Sorafenib groups), as well as HCCLM3 cells with control or CCN2 overexpression (designated as control and CCN2 groups), were subcutaneously injected into the left anterior axilla of female BALB/c nude mice to generate xenograft tumor models (n = 6 per group). Mice in the Sorafenib and shCCN2 + Sorafenib groups were administered 25 mg/kg sorafenib via intraperitoneal injection every three days, while control groups received an equivalent volume of saline. Tumor growth was monitored tri-weekly. Following a 30-day period, the mice were euthanized, and

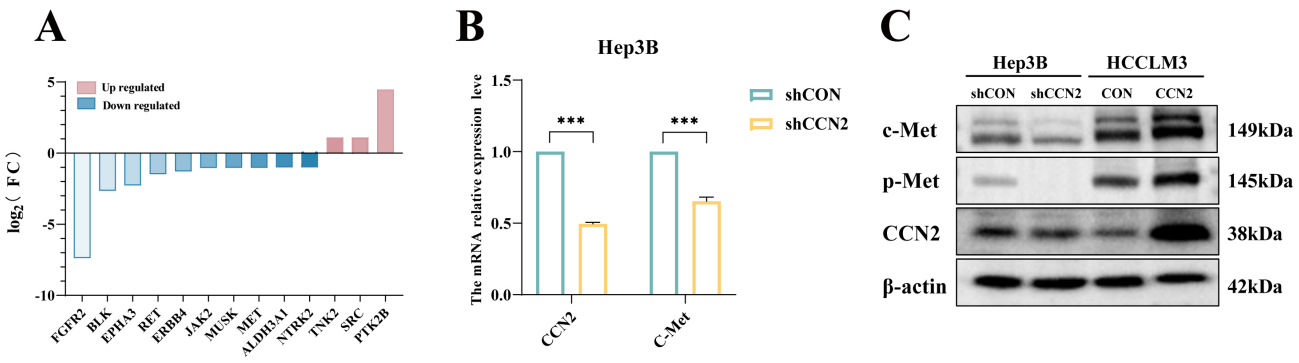

Fig. 3. CCN2 enhancing sorafenib resistance in hepatocellular carcinoma cells through activation of the c-Met signaling pathway. (A) Tyrosine kinase PCR array analysis. (B) RT-qPCR detection of changes in CCN2 and c-Met expression levels upon CCN2 knockdown. (C) Western blot analysis of changes in c-Met protein expression levels upon CCN2 knockdown or overexpression. ***$p < 0.001$.

the tumors were excised for volume and weight measurement (Fig. 5A–C). The results showed that tumors in the CCN2-overexpressing group were significantly larger than those in the control group (806.87 mm^3 vs. 502.49 mm^3). Critically, the shCCN2 + Sorafenib combination group exhibited the smallest tumor volume (135.10 mm^3), which was substantially reduced compared to the shCON (649.33 mm^3), Sorafenib-alone (353.59 mm^3), and shCCN2-alone (315.29 mm^3) groups (Fig. 5A,B). Corroborating this functional data, immunohistochemical analysis confirmed the involvement of the c-Met pathway: c-Met expression was significantly lower in the shCCN2 group than in the shCON group, and higher in the CCN2-overexpressing group compared to its control (Fig. 5D). Collectively, these findings indicate that CCN2 interference alleviates c-Met-mediated sorafenib resistance, and that combining sorafenib with CCN2 targeting enhances its antitumor efficacy.

4. Discussions

HCC remains one of the most prevalent and prognostically poor malignancies globally. With the evolving disease spectrum of HCC, identifying novel therapeutic targets and sensitive biomarkers for early diagnosis and improved treatment is increasingly urgent. Hepatocarcinogenesis involves a complex interplay of multiple oncogenes, tumor suppressor genes, and growth factors, where precise gene expression control is crucial for normal cellular function [23]. Against this backdrop, the CCN family matricellular protein CCN2 has garnered attention. Initially recognized for its roles in inflammation, injury response, and wound healing, aberrant CCN2 expression is an established biomarker for fibrotic diseases [9]. Notably, its dysregulation is also implicated in the development and progression of various malignancies, highlighting its significant clinical potential as a diagnostic and prognostic biomarker, as well as a promising therapeutic target.

CCN2 is one of six structurally related proteins defined by conserved domains and sequence homology. Structurally, it is a 349-amino acid protein comprising four modular domains: IGFBP (Module I), VWC (Module II), TSP1 (Module III), and CT (Module IV) [24,25]. Functionally, recent studies have elucidated several key biological roles of CCN2 [9,26–28]: namely, it (1) initiates signal transduction by binding receptors such as integrins, HSPGs, LRP, and tyrosine kinases; (2) modulates the availability and activity of cytokines; (3) interacts with ECM components like fibronectin, tenascin, and hyaluronan—interactions that are crucial for promoting cell adhesion, motility, and mediating ECM turnover during tissue remodeling; and (4) regulates crosstalk between signaling pathways while modulating the activity of various cytokines and growth factors. Transforming growth factor-beta (TGF-β) transcriptionally activates CCN2, promoting its secretion into the extracellular matrix and enhancing its cellular expression, thereby contributing to liver fibrosis [29]. Furthermore, CCN2 facilitates the differentiation of hepatic stellate cells into myofibroblasts and promotes liver carcinogenesis [30]. Supporting its pro-tumorigenic role, a study by Mazzocca A *et al*. [31] showed that downregulating CCN2 expression suppressed hepatocellular carcinoma growth, intravascular invasion, and metastasis by inhibiting the proliferation of tumor-associated fibroblasts. This study also correlated CCN2 expression levels with clinical parameters in liver cancer patients, including hepatitis B history, AST levels, cirrhosis severity, and tumor size. Furthermore, our experimental results revealed that CCN2 promotes the abnormal proliferation of HCC, indicating its significant role in the malignant progression of HCC. Interestingly, we also observed a potential association between CCN2 and HCC cell migration. However, this preliminary finding is based solely on a single cell line and a single experimental approach, warranting further in-depth investigation in future studies. In short, further investigation into CCN2's functions in hepatocarcinogenesis is valuable for elucidating the underlying molecular mechanisms. Targeting CCN2 therapeutically could thus be crucial for improving treatment outcomes and prognosis in HCC patients.

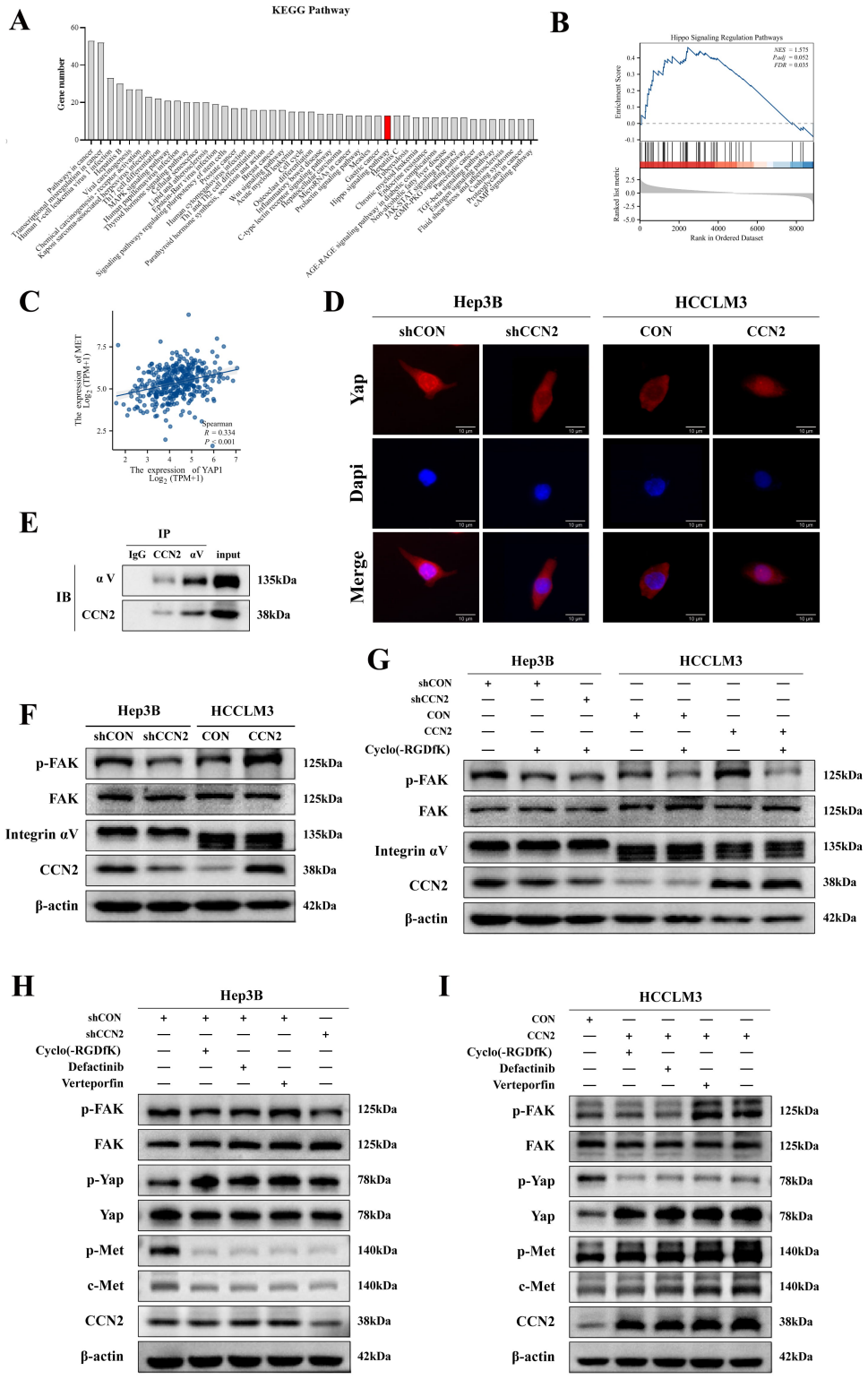

Fig. 4. CCN2 upregulating c-Met expression in hepatocellular carcinoma cells via integrin-mediated FAK/YAP activation. (A) Enrichment of c-Met transcription factor signaling pathways. (B) GSEA enrichment analysis indicating an association between CCN2 and Hippo Signaling Regulation Pathways. (C) Positive correlation between YAP and c-Met. (D) Immunofluorescence detection of YAP changes following CCN2 overexpression or knockdown. Scale bar: 10 μm. (E) Co-immunoprecipitation (Co-IP) analysis of the interaction between CCN2 and integrin αV. (F) Western blot analysis of FAK, p-FAK, and integrin αV expression changes following CCN2 overexpression or knockdown. (G) Treatment of LM3 cells overexpressing CCN2 with the integrin inhibitor Cyclo(-RGDfK) resulting in corresponding inhibition of FAK phosphorylation levels. (H,I) CCN2 upregulating c-Met expression via integrin-mediated FAK/YAP activation. FAK/YAP, focal adhesion kinase/yes-associated protein.

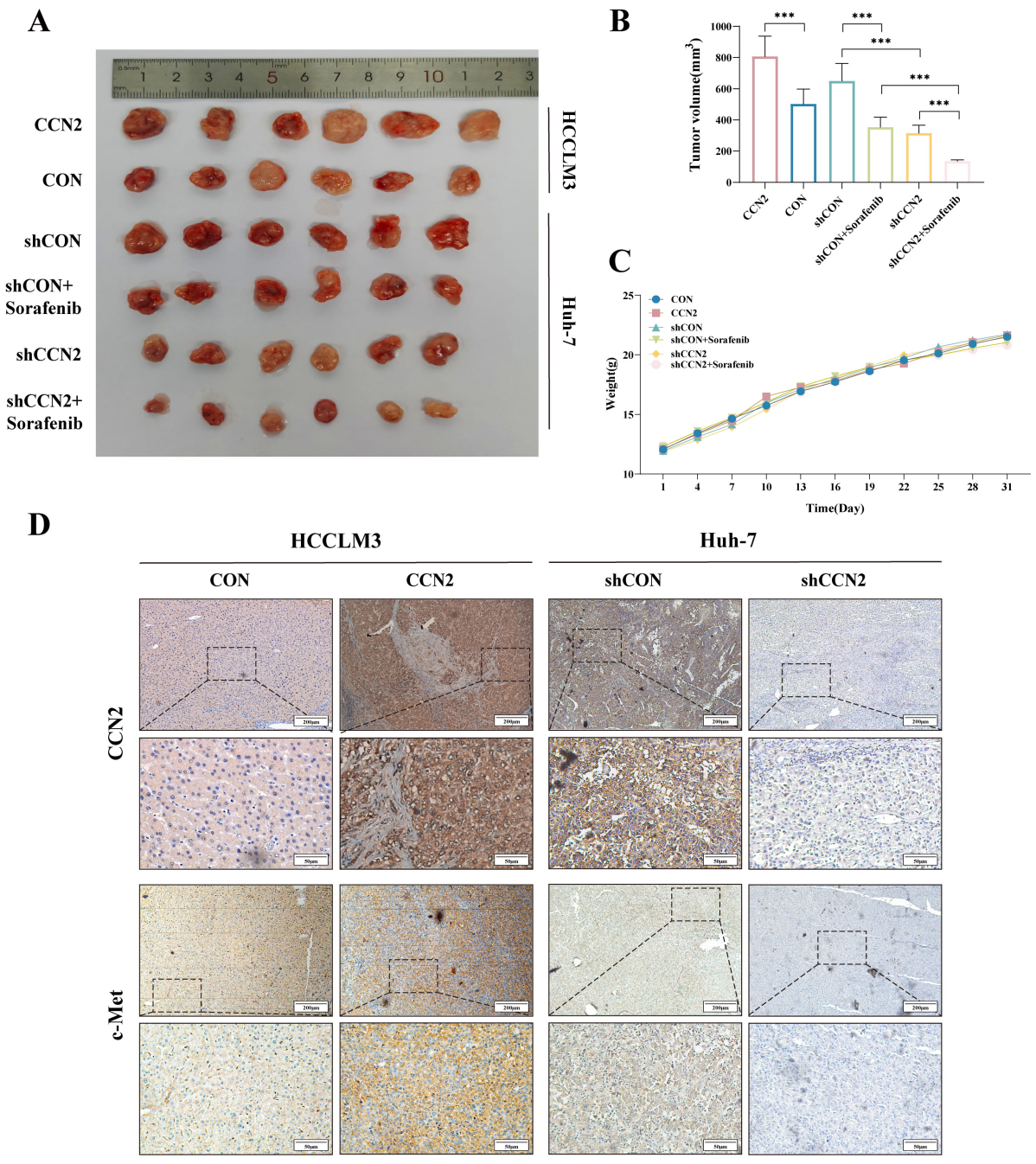

Fig. 5. ***In vivo*** **xenograft tumor study.** (A) Representative images of xenograft tumors after excision from each group (n = 6). (B) Changes in tumor volume across groups. (C) Trends in body weight of nude mice across groups. (D) Immunohistochemical detection of CCN2 and c-Met expression levels. Scale bar: 200 μm (upper) and 50 μm (lower). ***$p < 0.001$.

Sorafenib, a multi-kinase inhibitor, suppresses tumor growth primarily by targeting the RAF/MEK/ERK and PI3K/AKT/mTOR pathways to inhibit proliferation and angiogenesis. While effective in some patients, its clinical utility is often compromised by both intrinsic and acquired resistance. Phase III trials revealed that sorafenib extends overall survival by only 2–3 months in about 30% of HCC patients, with most developing resistance within six months and experiencing significant side effects [32,33]. Although multiple mechanisms—including dysregulated apoptosis, autophagy, epithelial-mesenchymal transition (EMT), cancer stem cells, the tumor microenvironment, and key signaling pathways—have been linked to this resistance, the underlying causes remain poorly defined. Given its ability to interact with various membrane receptors such as Met and integrins, CCN2 has emerged as a participant in tumor chemoresistance. Previous studies from our group have associated CCN2 overexpression with poor prognosis and oxaliplatin resistance in HCC, suggesting its potential role as a molecular marker of chemoresistance in HCC cells [17]. To investigate the functional role of CCN2, we performed sorafenib sensitivity assays, which demonstrated

that CCN2 silencing enhanced the susceptibility of hepatocellular carcinoma cells to this targeted agent. The combination of CCN2 knockdown and sorafenib treatment resulted in significantly suppressed tumor cell proliferation. Subsequent PCR array analysis of protein tyrosine kinases in CCN2-interfered cell lines revealed a pronounced reduction in mRNA expression, most notably in c-Met. This finding confirms that CCN2 abnormally activates the c-Met signaling pathway, which cooperatively drives HCC malignancy and confers sorafenib resistance. These results imply that in clinical practice, the aggressive behavior and poor sorafenib response observed in patients with high CCN2 expression may be mediated through CCN2-induced hyperactivation of the c-Met pathway.

The c-Met proto-oncogene, located on chromosome 7q21-31, encodes the receptor tyrosine kinase c-Met [34]. This protein regulates a network of downstream pathways—including Ras/Raf/MEK/MAPK, PI3K/AKT/mTOR, and JAK/STAT—thereby influencing key cellular processes such as proliferation, survival, migration, and angiogenesis [35]. Dysregulation of c-Met is frequently observed in multiple cancers, where its overexpression drives tumorigenesis and confers resistance to targeted therapies [36], notably in HCC, gastric cancer, and non-small cell lung cancer [37]. In HCC specifically, c-Met expression is significantly higher in tumor tissues compared to adjacent normal liver, underscoring its activation as a key contributor to sorafenib resistance. Furthermore, CCN2 overexpression has been shown to upregulate c-Met expression, and the MET/HGF pathway is known to promote proliferation and invasion in HCC cells. Consequently, our findings identify the tyrosine kinase c-Met as a critical effector molecule in CCN2-mediated sorafenib resistance.

Integrins, which are heterodimeric receptors composed of α and β subunits, promote tumor progression through mechanisms such as enhancing cancer stemness and activating survival/growth signaling pathways, either independently or in synergy with growth factor receptors [38]. Notably, the C-terminal domain of CCN2 contains a known binding site for integrin $\alpha v\beta 3$ [39]. To investigate this interaction in our experimental context, we confirmed the direct binding between CCN2 and the integrin αV subunit via co-immunoprecipitation. Furthermore, treatment with the integrin inhibitor Cyclo(-RGDfK) in CCN2-overexpressing HCC cells led to a corresponding decrease in FAK phosphorylation, functionally linking CCN2-integrin binding to downstream FAK pathway activation. Subsequent transcription factor enrichment analysis identified the Hippo signaling pathway as a major regulator of c-Met expression implicated in sorafenib resistance. The Hippo pathway, crucial for controlling organ size, cell proliferation, and apoptosis, is centrally mediated by the effectors YAP and TAZ [40]. YAP requires nuclear translocation to function as a transcriptional coactivator, a process known to be promoted upstream by FAK activation [41]. Building on this model, we found that CCN2 activates the FAK pathway via integrin signaling, which in turn induces YAP nuclear translocation and subsequent transcriptional upregulation of c-Met. Importantly, this mechanism was therapeutically relevant, as *in vivo* studies demonstrated that simultaneously targeting CCN2 and administering sorafenib significantly suppressed the growth of hepatocellular carcinoma xenografts.

In conclusion, while the secreted protein CCN2 is typically considered an indirect ligand facilitating tumor progression, this study demonstrates that combining CCN2 interference with sorafenib produces significant anti-tumor effects in liver cancer. Both *in vitro* and *in vivo* experiments established that CCN2 binds integrin αV, activating the FAK pathway, which in turn promotes YAP nuclear translocation and transcriptionally upregulates c-Met expression. The subsequent activation of c-Met downstream signaling ultimately mediates sorafenib resistance. Collectively, these findings unveil a novel mechanistic pathway underlying sorafenib resistance in HCC and provide a strong rationale for targeting CCN2 as a promising therapeutic strategy.

This study acknowledges several limitations that should be considered when interpreting the findings. First, the analysis of the association between CCN2 expression and the clinical characteristics of HCC patients was based solely on a retrospective design. Prospective studies are warranted to validate these observations and to incorporate longer-term patient follow-up data to clarify the relationship between CCN2 and HCC prognosis. Second, while this research offers preliminary insights into the role and mechanism of CCN2 in sorafenib resistance in HCC, the precise molecular interactions between CCN2 and the downstream integrin αV–FAK–YAP–cMet axis remain to be fully elucidated through further *in vitro* and *in vivo* experiments. Third, the link between CCN2 and HCC cell migration was observed using a single cell line and experimental approach. Although this provides a meaningful direction for future investigation, additional studies are necessary to comprehensively explore the role and underlying mechanisms of CCN2 in HCC metastasis.

5. Conclusions

Drawing from both the current findings and prior research, the following conclusions could be reached: (1) CCN2 correlates with the proliferation and migration of hepatocellular carcinoma cells; (2) c-Met, a tyrosine kinase, acts as an effector in the CCN2-mediated resistance to sorafenib; (3) CCN2's binding to integrin αV triggers the FAK signaling cascade downstream, wherein FAK's activation facilitates YAP's nuclear entry, leading to the transcriptional upregulation of c-Met and the subsequent activation of its downstream pathways, thereby mediating sorafenib resistance; and (4) the concurrent application of CCN2 interference and sorafenib markedly suppresses tumor growth and notably enhances the susceptibility of hepatocellular carcinoma cells to sorafenib.

Availability of Data and Materials

The data used to support the findings of this study are available from the corresponding author upon reasonable request.

Author Contributions

LC and JL conceived and designed the experiments, performed the experiments, prepared figures and tables, authored or reviewed drafts of the paper, and approved the final draft. YL and BC analyzed the data, prepared figures and tables, and approved the final draft. YB and KL conceived and designed the experiments, authored or reviewed drafts of the paper, and approved the final draft. All authors contributed to editorial changes in the manuscript. All authors read and approved the final manuscript. All authors have participated sufficiently in the work and agreed to be accountable for all aspects of the work.

Ethics Approval and Consent to Participate

This study followed the ethical standards of the Declaration of Helsinki. All experimental procedures involving animals were performed in strict accordance with the National Institutes of Health guidelines for the care and use of laboratory animals and were approved by the Medical Research Ethics Review Committee of the General Hospital of Ningxia Medical University (No. KLYY-2019-080). A written consent was signed by the patients or their families/legal guardians for the publication of anonymized clinical data and any potentially identifiable images included in this study. Consent documentation confirms understanding that: Clinical details and images will be used solely for scientific purposes. No financial compensation will be provided for data/image usage.

Acknowledgment

Not applicable.

Funding

This study was funded by the National Natural Science Foundation (No. 81960533), Natural Science Foundation of Ningxia Hui Autonomous Region (No. 2023AAC03507), Natural Science Foundation of Ningxia Hui Autonomous Region (No. 2023AAC03606), and Key R&D Program of Ningxia Hui Autonomous Region for High-level Talents Introduction (No. 2024BEH04154).

Conflict of Interest

The authors declare no conflict of interest.

Declaration of AI and AI-Assisted Technologies in the Writing Process

During the preparation of this manuscript, the authors used ChatGPT to assist with spelling and grammar checks in both the Introduction and Discussion sections. Following this, the authors carefully reviewed, edited, and refined the content as necessary. The authors take full responsibility for the accuracy and integrity of the published work.

Supplementary Material

Supplementary material associated with this article can be found, in the online version, at https://doi.org/10.31083/FBL45454.

References

[1] Bray F, Laversanne M, Sung H, Ferlay J, Siegel RL, Soerjomataram I, *et al*. Global cancer statistics 2022: GLOBOCAN estimates of incidence and mortality worldwide for 36 cancers in 185 countries. CA: a Cancer Journal for Clinicians. 2024; 74: 229–263. https://doi.org/10.3322/caac.21834.

[2] Han B, Zheng R, Zeng H, Wang S, Sun K, Chen R, *et al*. Cancer incidence and mortality in China, 2022. Journal of the National Cancer Center. 2024; 4: 47–53. https://doi.org/10.1016/j.jncc.2024.01.006.

[3] Zhang Y, Yue S, Zhang B, Chen X, Zhang W. Neoadjuvant systemic therapy for hepatocellular carcinoma: challenges and opportunities-a narrative review. Hepatobiliary surgery and nutrition. 2025; 14: 795–813. https://doi.org/10.21037/hbsn-24-175.

[4] Zeng H, Cao M, Xia C, Wang D, Chen K, Zhu Z, *et al*. Performance and effectiveness of hepatocellular carcinoma screening in individuals with HBsAg seropositivity in China: a multicenter prospective study. Nature Cancer. 2023; 4: 1382–1394. https://doi.org/10.1038/s43018-023-00618-8.

[5] Ganesan P, Kulik LM. Hepatocellular Carcinoma: New Developments. Clinics in Liver Disease. 2023; 27: 85–102. https://doi.org/10.1016/j.cld.2022.08.004.

[6] Haber PK, Puigvehí M, Castet F, Lourdusamy V, Montal R, Tabrizian P, *et al*. Evidence-Based Management of Hepatocellular Carcinoma: Systematic Review and Meta-analysis of Randomized Controlled Trials (2002–2020). Gastroenterology. 2021; 161: 879–898. https://doi.org/10.1053/j.gastro.2021.06.008.

[7] Galle PR, Dufour JF, Peck-Radosavljevic M, Trojan J, Vogel A. Systemic therapy of advanced hepatocellular carcinoma. Future Oncology (London, England). 2021; 17: 1237–1251. https://doi.org/10.2217/fon-2020-0758.

[8] Alawyia B, Constantinou C. Hepatocellular Carcinoma: a Narrative Review on Current Knowledge and Future Prospects. Current Treatment Options in Oncology. 2023; 24: 711–724. https://doi.org/10.1007/s11864-023-01098-9.

[9] Ramazani Y, Knops N, Elmonem MA, Nguyen TQ, Arcolino FO, van den Heuvel L, *et al*. Connective tissue growth factor (CTGF) from basics to clinics. Matrix Biology: Journal of the International Society for Matrix Biology. 2018; 68-69: 44–66. https://doi.org/10.1016/j.matbio.2018.03.007.

[10] Chu CY, Chang CC, Prakash E, Kuo ML. Connective tissue growth factor (CTGF) and cancer progression. Journal of Biomedical Science. 2008; 15: 675–685. https://doi.org/10.1007/s11373-008-9264-9.

[11] Ghosh P, Dey A, Nandi S, Majumder R, Das S, Mandal M. CTGF (CCN2): a multifaceted mediator in breast cancer progression and therapeutic targeting. Cancer Metastasis Reviews. 2025; 44: 32. https://doi.org/10.1007/s10555-025-10248-4.

[12] Zhou Z, Yan S, Zhang R, Wang H, Ye Z, Zhang Z, *et al*. CTGF/CCN2 promotes the proliferation of human osteosarcoma cells via cross-talking with the stromal CXCL12/CXCR4-AKT-αvβ3 signaling axis in tumor microenvironment. Genes & Diseases. 2022; 10: 356–358. https://doi.org/10.1016/j.gendis.2022.04.016.

[13] Zhang S, Li B, Tang W, Ni L, Ma H, Lu M, *et al*. Effects of

connective tissue growth factor on prostate cancer bone metastasis and osteoblast differentiation. Oncology letters. 2018; 16: 2305–2311. https://doi.org/10.3892/ol.2018.8960.

[14] Zheng M, Liu L, Cui H, Zhao Y, Chen W, Bai S, *et al*. Cancer-associated fibroblast-derived extracellular vesicles facilitate metastasis in hepatocellular carcinoma by delivering CTGF. Cellular Oncology (Dordrecht, Netherlands). 2025; 48: 1413–1432. https://doi.org/10.1007/s13402-025-01085-2.

[15] Tsai HC, Chang AC, Tsai CH, Huang YL, Gan L, Chen CK, *et al*. CCN2 promotes drug resistance in osteosarcoma by enhancing ABCG2 expression. Journal of Cellular Physiology. 2019; 234: 9297–9307. https://doi.org/10.1002/jcp.27611.

[16] Zeng H, Yang Z, Xu N, Liu B, Fu Z, Lian C, *et al*. Connective tissue growth factor promotes temozolomide resistance in glioblastoma through TGF-β1-dependent activation of Smad/ERK signaling. Cell Death & Disease. 2017; 8: e2885. https://doi.org/10.1038/cddis.2017.248.

[17] Liao X, Bu Y, Jiang S, Chang F, Jia F, Xiao X, *et al*. CCN2-MAPK-Id-1 loop feedback amplification is involved in maintaining stemness in oxaliplatin-resistant hepatocellular carcinoma. Hepatology International. 2019; 13: 440–453. https://doi.org/10.1007/s12072-019-09960-5.

[18] Fu J, Su X, Li Z, Deng L, Liu X, Feng X, *et al*. HGF/c-Met pathway in cancer: from molecular characterization to clinical evidence. Oncogene. 2021; 40: 4625–4651. https://doi.org/10.1038/s41388-021-01863-w.

[19] Park KC, Richardson DR. The c-Met oncoprotein: Function, mechanisms of degradation and its targeting by novel anticancer agents. Biochimica et Biophysica Acta. General Subjects. 2020; 1864: 129650. https://doi.org/10.1016/j.bbagen.2020.129650.

[20] Bahrami A, Shahidsales S, Khazaei M, Ghayour-Mobarhan M, Maftouh M, Hassanian SM, *et al*. C-Met as a potential target for the treatment of gastrointestinal cancer: Current status and future perspectives. Journal of Cellular Physiology. 2017; 232: 2657–2673. https://doi.org/10.1002/jcp.25794.

[21] Zhang H, Feng Q, Chen WD, Wang YD. HGF/c-Met: A Promising Therapeutic Target in the Digestive System Cancers. International Journal of Molecular Sciences. 2018; 19: 3295. https://doi.org/10.3390/ijms19113295.

[22] Tang W, Chen Z, Zhang W, Cheng Y, Zhang B, Wu F, *et al*. The mechanisms of sorafenib resistance in hepatocellular carcinoma: theoretical basis and therapeutic aspects. Signal Transduction and Targeted Therapy. 2020; 5: 87. https://doi.org/10.1038/s41392-020-0187-x.

[23] Wang Y, Deng B. Hepatocellular carcinoma: molecular mechanism, targeted therapy, and biomarkers. Cancer Metastasis Reviews. 2023; 42: 629–652. https://doi.org/10.1007/s10555-023-10084-4.

[24] Ren M, Yao S, Chen T, Luo H, Tao X, Jiang H, *et al*. Connective Tissue Growth Factor: Regulation, Diseases, and Drug Discovery. International Journal of Molecular Sciences. 2024; 25: 4692. https://doi.org/10.3390/ijms25094692.

[25] Perbal B. CCN proteins: multifunctional signalling regulators. Lancet (London, England). 2004; 363: 62–64. https://doi.org/10.1016/S0140-6736(03)15172-0.

[26] Luft FC. CCN2, the connective tissue growth factor. Journal of Molecular Medicine (Berlin, Germany). 2008; 86: 1–3. https://doi.org/10.1007/s00109-007-0287-x.

[27] Turner CA, Sharma V, Hagenauer MH, Chaudhury S, O'Connor AM, Hebda-Bauer EK, *et al*. Connective Tissue Growth Factor Is a Novel Prodepressant. Biological Psychiatry. 2018; 84: 555–562. https://doi.org/10.1016/j.biopsych.2018.04.013.

[28] Zaykov V, Chaqour B. The CCN2/CTGF interactome: an approach to understanding the versatility of CCN2/CTGF molecular activities. Journal of Cell Communication and Signaling. 2021; 15: 567–580. https://doi.org/10.1007/s12079-021-00650-2.

[29] Black SA, Jr, Trackman PC. Transforming growth factor-beta1 (TGFbeta1) stimulates connective tissue growth factor (CCN2/CTGF) expression in human gingival fibroblasts through a RhoA-independent, Rac1/Cdc42-dependent mechanism: statins with forskolin block TGFbeta1-induced CCN2/CTGF expression. The Journal of Biological Chemistry. 2008; 283: 10835–10847. https://doi.org/10.1074/jbc.M710363200.

[30] Gao R, Ball DK, Perbal B, Brigstock DR. Connective tissue growth factor induces c-fos gene activation and cell proliferation through p44/42 MAP kinase in primary rat hepatic stellate cells. Journal of Hepatology. 2004; 40: 431–438. https://doi.org/10.1016/j.jhep.2003.11.012.

[31] Mazzocca A, Fransvea E, Dituri F, Lupo L, Antonaci S, Giannelli G. Down-regulation of connective tissue growth factor by inhibition of transforming growth factor beta blocks the tumor-stroma cross-talk and tumor progression in hepatocellular carcinoma. Hepatology (Baltimore, Md.). 2010; 51: 523–534. https://doi.org/10.1002/hep.23285.

[32] Cersosimo RJ. Systemic targeted and immunotherapy for advanced hepatocellular carcinoma. American Journal of Health-System Pharmacy. 2021; 78: 187–202. https://doi.org/10.1093/ajhp/zxaa365.

[33] Cheng A, Kang Y, Chen Z, Tsao CJ, Qin S, Kim JS, *et al*. Efficacy and safety of sorafenib in patients in the Asia-Pacific region with advanced hepatocellular carcinoma: a phase III randomised, double-blind, placebo-controlled trial. The Lancet Oncology. 2009; 10: 25–34. https://doi.org/10.1016/S1470-2045(08)70285-7.

[34] Cooper CS, Park M, Blair DG, Tainsky MA, Huebner K, Croce CM, *et al*. Molecular cloning of a new transforming gene from a chemically transformed human cell line. Nature. 1984; 311: 29–33. https://doi.org/10.1038/311029a0.

[35] Moosavi F, Giovannetti E, Saso L, Firuzi O. HGF/MET pathway aberrations as diagnostic, prognostic, and predictive biomarkers in human cancers. Critical Reviews in Clinical Laboratory Sciences. 2019; 56: 533–566. https://doi.org/10.1080/10408363.2019.1653821.

[36] He M, Peng A, Huang XZ, Shi DC, Wang JC, Zhao Q, *et al*. Peritumoral stromal neutrophils are essential for c-Met-elicited metastasis in human hepatocellular carcinoma. Oncoimmunology. 2016; 5: e1219828. https://doi.org/10.1080/2162402X.2016.1219828.

[37] Sivakumar M, Jayakumar M, Seedevi P, Sivasankar P, Ravikumar M, Surendar S, *et al*. Meta-analysis of functional expression and mutational analysis of c-Met in various cancers. Current Problems in Cancer. 2020; 44: 100515. https://doi.org/10.1016/j.currproblcancer.2019.100515.

[38] Hamidi H, Ivaska J. Every step of the way: integrins in cancer progression and metastasis. Nature Reviews. Cancer. 2018; 18: 533–548. https://doi.org/10.1038/s41568-018-0038-z.

[39] Wang YK, Weng HK, Mo FE. The regulation and functions of the matricellular CCN proteins induced by shear stress. Journal of cell communication and signaling. 2023; 17: 361–370. https://doi.org/10.1007/s12079-023-00760-z.

[40] Moya IM, Halder G. Hippo-YAP/TAZ signalling in organ regeneration and regenerative medicine. Nature Reviews. Molecular Cell Biology. 2019; 20: 211–226. https://doi.org/10.1038/s41580-018-0086-y.

[41] Song X, Xu H, Wang P, Wang J, Affo S, Wang H, *et al*. Focal adhesion kinase (FAK) promotes cholangiocarcinoma development and progression via YAP activation. Journal of Hepatology. 2021; 75: 888–899. https://doi.org/10.1016/j.jhep.2021.05.018.